Published in final edited form as:
Neuroimage. 2013 August 15; 77: 93–104. doi:10.1016/j.neuroimage.2013.03.049.

The scent of salience — Is there olfactory-trigeminal conditioning in humans?

C. Moessnang[a,b,*], **K. Pauly**[a,b], **T. Kellermann**[a,b], **J. Krämer**[a,b], **A. Finkelmeyer**[c], **T. Hummel**[d], **S.J. Siegel**[e], **F. Schneider**[a,b], and **U. Habel**[a,b]

C. Moessnang: camoessnang@ukaachen.de; K. Pauly: kpauly@ukaachen.de; J. Krämer: jkraemer@ukaachen.de; A. Finkelmeyer: andreas.finkelmeyer@newcastle.ac.uk; T. Hummel: thummel@mail.zih.tu-dresden.de; S.J. Siegel: siegels@exchange.upenn.edu

[a]Department of Psychiatry, Psychotherapy and Psychosomatics, RWTH Aachen University, Pauwelsstraße 30, 52074 Aachen, Germany

[b]JARA Translational Brain Medicine, Jülich/Aachen, Germany

[c]Institute of Neuroscience, Newcastle University, Framlington Place, Newcastle Upon Tyne, England, UK

[d]Department of Otorhinolaryngology, University of Dresden, Medical School, 01307 Dresden, Germany

[e]Department of Psychiatry, Translational Research Laboratory, University of Pennsylvania, 125 S 31st Street, Philadelphia, PA 19104, USA

Abstract

Pavlovian fear conditioning has been thoroughly studied in the visual, auditory and somatosensory domain, but evidence is scarce with regard to the chemosensory modality. Under the assumption that Pavlovian conditioning relies on the supra-modal mechanism of salience attribution, the present study was set out to attest the existence of chemosensory aversive conditioning in humans as a specific instance of salience attribution. fMRI was performed in 29 healthy subjects during a differential aversive conditioning paradigm. Two odors (rose, vanillin) served as conditioned stimuli (CS), one of which (CS+) was intermittently coupled with intranasally administered CO_2. On the neural level, a robust differential response to the CS+ emerged in frontal, temporal, occipito-parietal and subcortical brain regions, including the amygdala. These changes were paralleled by the development of a CS+-specific connectivity profile of the anterior midcingulate cortex (aMCC), which is a key structure for processing salience information in order to guide adaptive response selection. Increased coupling could be found between key nodes of the salience network (anterior insula, neo-cerebellum) and sensorimotor areas, representing putative input and output structures of the aMCC for exerting adaptive motor control. In contrast, behavioral and skin conductance responses did not show significant effects of conditioning, which has been attributed

*Corresponding author at: Department of Psychiatry, Psychotherapy and Psychosomatics, RWTH Aachen University, Pauwelsstrasse 30, 52074 Aachen, Germany. Fax: +49 241 80402.

Confiict of interest

Authors declare no confiict of interests.

Supplementary data to this article can be found online at http://dx.doi.org/10.1016/j.neuroimage.2013.03.049.

to contingency unawareness. These findings imply substantial similarities of conditioning involving chemosensory and other sensory modalities, and suggest that salience attribution and adaptive control represent a general, modality-independent principle underlying Pavlovian conditioning.

Keywords

Chemosensation; Pavlovian conditioning; Salience; Functional connectivity; fMRI

Introduction

Pavlovian fear conditioning and its neural correlates have been well described in the visual, auditory and somatosensory modality (for review, see Sehlmeyer et al., 2009), but only little is known about aversive conditioning within the chemical senses in humans. Given the evolutionary significance of the chemosensory system across species (Shepherd 2004), one might speculate equal or even better associative learning within this system.

Only one EEG study has been performed in which olfactory CS were paired with a painful trigeminal US (Bensafi et al., 2007). Conditioned behavioral and electrophysiological responses (CR) were only found in a subset of subjects. Together with other behavioral (e.g. Busch and Evans, 1977; Marinkovic et al., 1989; Todrank et al., 1995) and EEG studies (Hermann et al., 2000) involving at least one chemosensory stimulus, these findings suggest that aversive conditioning in the chemosensory domain is more subtle and less robust than in other sensory modalities.

This interpretation, which is presumably premature given the limited number of studies, is challenged by the assumption of a general, modality-independent learning mechanism which might underlie Pavlovian conditioning and which is supported by abundant evidence of successful conditioning involving stimuli of different modalities (see Sehlmeyer et al., 2009). A promising candidate mechanism is the attribution of salience. Theoretical approaches of Pavlovian conditioning, such as the Rescorla–Wagner model (Rescorla, 1988), describe salience as “attention-gettingness” of the CS, which is positively correlated with its proneness to become associated with the US, and which can change as a function of repeated pairing with the US (Rescorla, 1988). Here, salience is defined more broadly as the property of a stimulus to challenge the organism’s homeostasis, which in turn requires the initiation of an appropriate action (Seeley et al., 2007; Sterzer and Kleinschmidt, 2010). This definition of salience includes many different forms, ranging from unexpected changes in stimulus characteristics (e.g. novelty, which automatically elicits an orienting response), to stimuli with inherently motivational value (e.g. pain, which immediately elicits a defensive reaction). In this regard, Pavlovian conditioning can be viewed as a modality-independent process which involves the attribution of salience to a previously neutral CS due to repeated pairing with a highly salient stimulus (US), which in turn induces the initiation of an appropriate action (i.e. conditioned response). In other words, the CS becomes a predictor of the US, and therefore gains salience. This conceptualization of conditioning has already been adopted in studies on appetitive learning in humans (i.e. Heinz and Schlagenhauf,

2010; Jensen et al., 2008; Roiser et al., 2009), and on aversive learning in mice (Moessnang et al., 2012). The process of salience attribution should therefore apply to Pavlovian conditioning involving chemosensory stimuli as well.

The neural correlates of salience attribution and response initiation have recently been described using a network perspective approach (Seeley et al., 2007). Within this framework, the anterior insula (AI) and the adjacent opercular and inferior frontal cortex constitute a “hub” for salience detection, with major input from sensory, limbic and prefrontal areas (Cauda et al., 2011). A second network node is located in the dorsal anterior cingulate cortex (dACC) and is involved in adaptive response initiation, with major output to areas implicated in attentional and motor control (Beckmann et al., 2009). Based on a more recent cytoarchitectonic parcellation of the cingulate (Vogt, 2005), this network node seems to overlap with the so-called anterior midcingulate cortex (aMCC), which shares important functions related to the salience network. According to the ‘adaptive control hypothesis’ (Shackman et al., 2011), the aMCC is a convergence site of information about reinforcers, i.e. highly salient stimuli, which is used for response selection and initiation. In accordance with this idea, most robust activation of the aMCC has been reported during tasks which elicit aversively motivated behavior, such as during anticipation and delivery of pain (Drabant et al., 2011; Farrell et al., 2005) as well as during Pavlovian fear conditioning (Mechias et al., 2010). No study, however, has explicitly linked Pavlovian conditioning to the salience network.

The present study was therefore set out to answer two research questions. One aim was to establish olfactory-trigeminal conditioning in the fMRI environment and to extensively characterize conditioning effects on a neural (whole-brain), behavioral and physiological level. For this purpose, relatively selective olfactory stimuli were used as CS, and intranasally administered CO_2, which elicits painful, stinging sensations conveyed by the trigeminal nerve, was used as US. Based on conditioning studies involving other sensory modalities, effects on the neural level were expected in insular and frontal cortices, aMCC, primary sensory cortex (i.e. primary olfactory cortex, POC) and amygdala (Sehlmeyer et al., 2009). On an autonomous and behavioral level, successful conditioning should be reflected in altered skin conductance responses (SCR), as well as valence and intensity ratings. The second aim of our study was to characterize the processes underlying Pavlovian conditioning in the framework of salience attribution and adaptive control using a network perspective approach. More precisely, we anticipated increased CS-specific functional connectivity between aMCC and the AI as a result of conditioning, implying successful olfactory salience attribution. On a behavioral level, increased adaptive control could result in faster reaction times in response to the US when preceded by the CS.

Material and methods

Sample

Thirty-three right-handed (Edinburgh Inventory; Oldfield, 1971) volunteers participated in the study. Due to technical problems during fMRI scanning, four subjects had to be excluded from further analysis, leaving a final sample of 29 subjects (15 females; mean age 31.4 ± 9.6 years). Exclusion criteria related to impaired olfactory functioning or to structural

or functional changes in the brain encompassed acute or chronic disorders in the maxillary or frontal sinuses, intake of psychoactive substances or medication influencing olfaction, a history of neurological disorders, as well as a history of mental illness (the latter was assessed by the Structured Clinical Interview for DSM-IV Axis I Disorders SCID-I; Wittchen et al., 1997). Self-reported depressive symptoms were administered with the Beck Depression Inventory BDI-II (Hautzinger et al., 2006). Normal olfactory functioning was ensured by psychophysical testing using the Sniffin' Sticks Screening test (Hummel et al., 2001). The study was approved by the local ethics committee at the Faculty of Medicine, RWTH Aachen University, and conducted according to the Code of Ethical Principles for Medical Research involving human subjects of the World Medical Association (Declaration of Helsinki). All subjects gave written informed consent and received a compensation of 10 Euros per hour.

Experimental procedure

In a separate acclimation session outside the scanner, subjects were accustomed to the task and the olfactory setup and trained to breathe evenly through the mouth while avoiding nasal air flow (velopharyngeal closure). Psychopathological and psychophysical screenings were administered between acclimation session and fMRI experiment. During scanning, subjects were exposed to an olfactory-trigeminal conditioning paradigm. Finally, a post-scanning questionnaire was used to assess perceived stimulus characteristics and contingencies.

Chemosensory stimulation

Chemosensory stimuli were delivered by means of a computer controlled olfactometer (OM6b, Burghart Messtechnik GmbH, Wedel, Germany), which allowed for standardized olfactory stimulation in the absence of tactile or thermal cues. Nostrils were stimulated via two separate tubes ending in nose-pieces inserted into both nostrils. Continuous airflow through each tube was held constant at 8 l/min and heated close to body temperature. Onset and duration of chemosensory events were controlled by Presentation software (Neurobehavioral Systems, Albany, US). All chemical components were obtained at Sigma-Aldrich GmbH, Deisendorf, Germany. For olfactory stimulation, phenyl ethyl alcohol (rose odor) and vanillin were each mixed with propylene glycole, an odorless solvent, in a ratio of 1:10. Both odors are perceived as mildly pleasant and are known to act as a relatively selective odorant in reasonably low concentrations (Doty et al., 1978; Frasnelli et al., 2011). Intranasally administered carbon dioxide (CO_2) was used for trigeminal stimulation, which is odorless and leads to a stinging, painful sensation at a certain concentration. For technical reasons, odors were presented to the right nostril, whereas CO_2 was presented to the left nostril. Chemosensory stimuli were embedded in the continuous air stream at pre-defined ratios. These ratios were obtained during the acclimation session, where concentrations were individually adjusted using a step-wise procedure (see Supplementary material). Final concentrations were rated as "well perceivable" for both odors, and "unpleasant, but tolerable" for CO_2. On average, vanillin was presented at a mean concentration of 60.3 (±13.6) % v/v, rose with 53.6 (±14.8) % v/v, and CO_2 with 65.6 (±18.1) % v/v of total airflow. In order to counteract habituation and to maintain CO_2 aversiveness, subjects' responses (i.e. button press) to the CO_2 were monitored within a 3 s time window after CO_2 onset during the later experiment. CO_2 concentration was raised in steps of 0.5 l/min if

subjects committed two omissions in a row. This procedure ensured individually adjusted pain stimulation and therefore allowed for controlling for subjective pain sensitivity. On average, CO_2 concentration was raised by 2.5 (±2.2) steps, and final concentration amounted to 80.6 (±11.8) % v/v.

Conditioning procedure

During MR scanning, one odor (CS+) was intermittently coupled with the painful CO_2 (US) in 60% of trials, whereas the other (CS −) was never coupled with the US, resulting in three CS conditions: CS+_US, CS+, and CS−. The intermittent reinforcement schedule allowed for a US-free comparison of both CS. In addition, a US-only condition was introduced in order to assess the effect of pure trigeminal stimulation. The assignment of odors to CS conditions was reversed in two versions. Due to exclusion of subjects, 58% of subjects were measured with vanillin and 42% with rose as CS+. The total number of trials per condition was chosen according to the rationale of 1) maximizing the number of trials in conditions of interest (i.e. CS+, CS−), 2) keeping a comparable balance of the number of odor presentations (i.e. rose vs. vanillin) despite an intermittent coupling rate of 60%, 3) ensuring a sufficient number of CS+_US pairings, and 4) minimizing the total length of the experiment. Therefore, the odor assigned to CS+ trials was presented 40x in the CS+_US condition, and 30x in the CS+-only condition, resulting in a total of 70 presentations, whereas the odor assigned to the CS− condition was presented 45x. These outcome probabilities ($p(US|CS+) = 0.57$, $p(US|CS-) = 0$) were similar to those which have been used successfully in previous studies on conditioning (e.g. Büchel et al., 1999; Dunsmoor et al., 2007; Gottfried et al., 2002; Morris et al., 2001; Spoormaker et al., 2011). Finally, the US-only condition was presented 15x (Fig. 1).

In order to ensure sufficient commitment to the task and to monitor perceived stimulus characteristics, subjects were asked to rate the previous chemosensory event in 66% of trials regarding odor valence or intensity in CS conditions and aversiveness in US conditions. Rating scales were continuous, ranging from “not perceivable” to “too intense” or “too painful” for intensity and aversiveness, respectively, and from “very unpleasant” to “very pleasant” for valence. Poles were randomly reversed from trial to trial in order to maximize trial-specific rating. Rating was performed by moving a bar along a continuous scale, using the buttons of an fMRI compatible response device (LUMI-touch™, Lightwave Technologies, Richmond, Canada) placed under the right index and middle finger. The experiment was performed in two equally long sessions (session 1, session 2), with a short break of 2 to 5 min between sessions. This break served as a clear demarcation between the first and second sessions for later analysis, and allowed subjects to have a short rest. Trials were presented in a pseudo-randomized order with the restriction of no more than two identical conditions in a row. Each trial consisted of 1) a baseline (1500 ms, plus a jitter of 0 to 1500 ms, varied in 500 ms steps), 2) a pre-event phase (1500 ms), indicated by the color change of a centrally presented fixation cross from white to gray, which informed subjects about the forthcoming olfactory stimulation; 3) an event phase (500 to 1500 ms), where the chemosensory event was presented; and 4) an ISI (3000 s), which was followed by a 5) rating phase (5500 ms) in 66% of trials. Chemosensory events were presented during the event phase of the trial (see Fig. 1), and consisted of a 1000 ms odor pulse for CS− and CS+

conditions, which was followed by a 200 ms CO_2 pulse after a 300 ms inter-stimulus interval for CS+ _US conditions. A single 500 ms CO_2 pulse was presented in US-only conditions. The reason for using a shorter CO_2-duration in CS+_US trials relates to the finding that trigeminal stimuli are perceived as more intense when accompanied by odors (Livermore et al., 1992). Subjects were instructed to pay attention to the odors. They were also told to quickly press the button with their right index finger upon CO_2 detection to avoid an increase of CO_2 concentration. Besides keeping track of individual pain sensitivity, as stated above, this manipulation allowed for inclusion of a behavioral measure of adaptive control. Subjects were told that the US could appear "anytime" during the experiment. No information was given about stimulus contingencies, and subjects' attention was not directed to a potential stimulus relationship. After fMRI scanning, subjects were given a questionnaire in which they were asked to give a summary rating of odor intensity and CO_2 aversiveness. They were also asked whether they perceived any association between odor and CO_2.

Data acquisition

Imaging parameters—Functional MRI was performed on a 3 T Tim Trio MR Scanner (Siemens, Erlangen, Germany) at the Department of Psychiatry, Psychotherapy, and Psychosomatic Medicine at the Hospital of the RWTH Aachen University. Functional images were collected in two runs with an echo-planar imaging (EPI) T2*-weighted contrast sequence sensitive to blood oxygenation level dependent (BOLD) changes (echo time [TE] = 30 ms, repetition time [TR] = 2 s, flip angle [α]: 76°, voxel size: 3.1 × 3.1 × 3.3 mm^3, 64 × 64 matrix, field of view [FOV]: 200 × 200 mm^2, slice thickness: 3.3 mm, gap: 0.6 mm, number of slices: 33 axial slices, whole-brain, slice acquisition sequence: ascending, 450 volumes per run).

Electrophysiology — skin conductance response (SCR)—Skin conductance data were assessed during the conditioning paradigm. Two silver–silver chloride (Ag–AgCl) electrodes were placed at the middle phalanges of the index and middle fingers of the left hand. The recording sites were prepared using an abrasive cleaning paste (Everi, Wetzlar, Germany), and electrodes were carefully filled with electrode gel (Biopac Systems, Goleta, USA). SCR data were recorded at a sampling rate of 5000 Hz in DC mode using a bipolar BrainAmp ExG MR amplifier (Brain Products, Gilching, Germany). Data were analyzed offline, including downsampling to 5 Hz, artifact reduction using spline interpolation, and extraction of phasic components from tonic activity based on continuous decomposition analysis (Benedek and Kaernbach, 2010) implemented in Ledalab© software. Data were normalized using a log transformation (y = log10(x + 1)) prior to statistical analysis.

Data analysis

Behavioral analysis—As successful conditioning should be reflected in the emergence of a differential response to CS+ and CS− in session 2, the main focus was set on the respective time × condition interaction. Continuous rating scales were transformed into scales ranging from 0 ("not perceivable") to 1 ("too intense/painful") for intensity and aversiveness, and from —1 ("very unpleasant") to 1 ("very pleasant") for valence. Mean valence and intensity ratings were entered into a 3 × 2-way repeated measures analysis of variance (rmANOVA),

with “condition” (CS+_US, CS+, CS−) and “session” (session 1 vs. session 2) as within-subjects factors. Median response times and mean response accuracy to CO_2 were analyzed in a 2 × 2-way rmANOVA, with “condition” (CS+_US vs. US) and “session” (session 1 vs. session 2) as within-subject factors. In addition, button presses in response to CS+ and CS− were analyzed as a measure of false alarms, using a 2 × 2-way rmANOVA with “condition” (CS+ vs. CS−) and “session” (session 1 vs. session 2) as within-subject factors. Finally, US aversiveness ratings, averaged across sessions, were analyzed in a one-sample *t*-test against a rating score of 0.5 (“moderately aversive”) in order to verify significant aversiveness of the US. Significance levels for repeated-measures analyses of variance (rmANOVA) were set to $p < .05$. If applicable, *t*-tests were calculated post-hoc as paired-sample *t*-tests, and Bonferroni correction for multiple comparisons was applied. Statistical calculations were performed with SPSS 17.0 (SPSS Inc., Chicago, US). Finally, post-scanning ratings were analyzed qualitatively. Average intensity and aversiveness ratings were calculated.

Analysis of SCR—SCR data of seven subjects had to be discarded due to technical failure. Phasic SCR responses were defined as deflections above 0.02 μS and were analyzed with respect to the parameters “nSCR” (number of SCRs) and “Amp” (amplitude measure derived from phasic driver activity) in a time window of 2–10 s after stimulus onset, as well as “%SCR” (percent trials with above-threshold SCR). Non-responders were defined as subjects that showed above-threshold SCR modulation in less than 20% of trials across conditions and sessions. This criterion was met by five subjects, leaving a total sample of n = 17 SCR datasets. In responders, individual session-wise means were subjected to a 4 × 2-way rmANOVA with within-subject factor “condition” (CS+_US, CS−, CS−, US) and “session” (session 1 vs. session 2).

Functional image analysis—Imaging data were analyzed using SPM8 (Statistical Parametric Mapping, Welcome Trust Centre for Neuroimaging, London, UK). Functional data were spatially preprocessed, including realignment, coregistration of the mean image into MNI space and normalization by means of unified segmentation (Ashburner and Friston, 2005), resulting in a voxel size of $1.5 \times 1.5 \times 1.5\ mm^3$, and spatial smoothing with an 8 mm full-width at half-maximum Gaussian Kernel. No subject had to be removed due to excessive motion (>3 mm).

Each chemosensory event (CS+, CS+_US, CS−, US) and the pre-event phase (PRE) were modeled as event-related regressors by convolution of the corresponding delta function with the canonical hemodynamic response function (HRF). The rating phase was modeled using a 5.5-s box car function which was also convolved with the canonical HRF. Realignment parameters were included as covariates of no interest. A high-pass filter with a period of 128 s was applied during parameter estimation by means of the general linear model (GLM). Effects were calculated for each session separately by contrasting the corresponding regressor to the implicit baseline. These contrasts were entered into a mixed-effects GLM for group-level inference, with subjects as random effects and conditions as fixed effects. For validation purpose, we report the following two contrasts in the supplement: An F-contrast over all events (CS−, CS+, CS+_US, US) in order to assess the main effect of chemosensory stimulation, and a t-contrast (PRE vs. baseline) in order to assess the impact

of the preceding pre-event phase on brain activation, both averaged across both sessions (see Supplementary results, Tables S1, S2, Figs. S1, S2).

A second GLM was calculated to assess the effect of CS conditions as a function of time. For this purpose, a 2 × 2-way ANOVA was calculated, with the within-subject factors "condition" (CS+ vs. CS−) and "session" (session 1 vs. session 2). Only voxels showing a modulation of the time × condition interaction at a threshold for $p_{uncorr} = .001$ were considered for further analysis. For this reason, differential brain activation to CS+ and CS− in each session, which was calculated using t-contrasts ($CS+_{sess1} > CS-_{sess1}$, $CS-_{sess1} > CS+_{sess1}$, $CS+_{sess2} > CS-_{sess2}$, $CS-_{sess2} > CS+_{sess2}$), was inclusively masked with the F contrast of the interaction term ($[CS+_{sess1} > CS-_{sess1}] < [CS+_{sess2} > CS-_{sess2}]$). The significance level for all reported activations was set to $p_{corr} < .05$, family-wise error (FWE) corrected for multiple comparisons across voxels (extent threshold: 50 voxels). A cytoarchitecture-based anatomical labeling of identified regions was performed by means of maximum probability maps provided the SPM Anatomy toolbox (www.fz-juelich.de/ime/spm_anatomy_toolbox, V1.8; Eickhoff et al., 2006a). The following maps were used in the present study, and are reported in detail elsewhere: primary somatosensory areas (3a, 3b, 1, 2; Geyer et al., 1999; Grefkes et al., 2001), secondary somatosensory areas (OP1-4; Eickhoff et al., 2006b), primary motor cortex (4a, 4p; Geyer et al., 1996), premotor cortex (BA6; Geyer, 2004), intraparietal sulcus (hIP1-3; Choi et al., 2006); superior parietal areas (7A, 7PC; Scheperjans et al., 2008), inferior parietal areas (PFop, PFt, PF, PFm, PFcm, PGa; Caspers et al., 2006), extrastriate visual areas (V3v, V4, V5/hOc3v, hOc4v, hOC5; Malikovic et al., 2007; Rottschy et al., 2007), cerebellum (Diedrichsen et al., 2009). Regions not covered by probability maps were reported according to the MNI-based AAl (Anatomical Automatic Labeling) database, implemented in SPM (Tzourio-Mazoyer et al., 2002).

Region of interest analysis—As significant time × condition interaction was expected in the POC and amygdala based on previous findings on Pavlovian conditioning (see Introduction), structurally defined ROIs were selected from the AAL database implemented in the SPM toolbox MarsBaR (http://marsbar.sourceforge.net) for each hemisphere. For each ROI, session-wise percent signal change was calculated and subjected to a 2 × 2-way rmANOVA, with within-subject factors "condition" (CS+ vs. CS−) and "session" (session 1 vs. session 2), and paired *t*-test were calculated post-hoc, using Bonferroni correction for multiple comparisons.

Psychophysiological interaction—Salience attribution was also explored using a network perspective approach. As the aMCC showed a robust differential response to both CS in session 2 in the group analysis (see Results), and is assumed to represent a key node of the salience network (see Introduction), the CS-specific functional connectivity of the aMCC was modeled during the first and second sessions using a psychophysiological interaction (PPI). Volumes of interest (VOI) were defined within the aMCC, which was guided by group-level statistics as follows: search volume was anatomically restricted by a mask consisting of a 10 mm sphere around the peak voxel at [8 23 29] that displayed significant differential activation in response to CS+ in the second session, using the t-

contrast outlined above ($CS+_{sess2} > CS-_{sess2}$; see Results). On the single subject level, individual VOIs were then defined in CS+-involving contrasts as supra-threshold voxels ($p_{uncorr} < .05$) within this mask. For each session, time courses were extracted from VOIs as the first eigenvariate, and adjusted for the session-specific effects of interest. A PPI regressor was generated as element-by-element product of the CS condition (psychological regressor: CS+, CS−) and the VOI time course (physiological regressor). A first-level GLM was estimated for each session and CS condition, including these three regressors as well as all remaining task-related regressors as described above. On the group level, connectivity patterns of the aMCC were analyzed in two ways. In order to assess the *task-independent*, i.e. non-differential connectivity patterns of the aMCC during the first and second sessions, VOI time courses were entered into a mixed-effects GLM, with subjects as random effects, and session-wise time courses as fixed effects. Differences in connectivity patterns between sessions were explored using t-contrasts (sess1 > sess2, sess2 > sess1). In a second step, the *task-dependent*, i.e. differential connectivity profile for CS+ and CS−trials was calculated by subjecting contrast estimates of the first- and second-session PPI regressors into a mixed-effects GLM, with subjects as random effects, and PPIs as fixed effects, yielding a 2 × 2-way ANOVA with within-subject factors “condition” (CS+ vs. CS−) and “session” (session 1 vs. session 2). Following the same rationale as in the analysis of task-induced brain activation (see above), differential connectivity of the aMCC within each session was explored using t-contrasts (PPI $CS+_{sess1}$ > PPI $CS-_{sess1}$, PPI $CS-_{sess1}$ > PPI $CS+_{sess1}$, PPI $CS+_{sess2}$ > PPI $CS-_{sess2}$, PPI $CS-_{sess2}$ > PPI $CS+_{sess2}$), which were inclusively masked by the interaction term ([PPI $CS+_{sess1}$ > PPI $CS-_{sess1}$] < [PPI $CS+_{sess2}$ > PPI $CS-_{sess2}$]). Due to a general lack of power of PPI analyses in event-related designs (O’Reilly et al., 2012), which is even more pronounced in the case of direct comparison of PPI models, a rather liberal statistical threshold of $p_{uncorr} < .001$ at voxel-level (extent threshold: k = 50 voxels) was used (with $p_{uncorr} < .05$ for the masking interaction term). However, to ensure sufficient control for false-positives, we employed a cluster-correction threshold at $p_{corr} < .05$, FWE corrected for multiple comparisons.

Results

Behavior

Analysis of intensity and valence ratings yielded a main effect of condition (intensity: $F_{[2,56]} = 14.55$, $p < .001$; valence: $F_{[2,56]} = 23.05$, $p < .001$, Fig. 2A). Post-hoc *t*-tests revealed higher intensity and lower valence ratings of the CS+_US condition compared to CS+ (intensity: $t_{[28]} = 4.86$, $p_{corr} < .001$; valence: $t_{[28]} = 5.90$, $p_{corr} < .001$) and CS− condition (intensity: $t_{[28]} = 3.39$, $p_{corr} = .006$; valence: $t_{[28]} = 4.54$, $p_{corr} < .001$) as a result of the concomitant trigeminal stimulation. No difference was found between the purely olfactory conditions CS+ and CS−. Analysis of US ratings confirmed sufficient aversiveness throughout the experiment when compared to the cutoff-score of 0.5 (“moderately aversive”, with a mean of 0.66 (±0.15); $t_{[28]} = 5.83$, $p < .001$). Finally, response times to the CO_2 showed a main effect of session ($F_{[1,27]} = 34.23$, $p < .001$), with faster responses in the second compared to the first session ($t_{[28]} = 5.85$, $p_{corr} < .001$). In contrast, a main effect of condition emerged for response accuracy ($F_{[1,27]} = 15.16$, $p = .001$), as subjects committed less omissions in unimodal US trials compared to bimodal CS+_US trials ($t_{[28]} = 3.89$, p_{corr}

= .001). The false alarm rate in response to CS+ and CS− was close to zero (overall mean: 2.32 (±0.62) %, and did not change as a function of condition or session (all $F_{[1,28]} < 0.96$, all $p > .337$). All mean values are reported in Table S3.

Skin conductance response

A significant impact of condition could be found for each SCR parameter (%SCR: $F_{[3,48]} = 42.27$, $p < .001$; Amp: $F_{[3,48]} = 19.63$, $p < .001$; nSCR: $F_{[3,48]} = 55.48$, $p < .001$), with increased SCR responses to CS+_US and US compared to purely olfactory CS conditions (all $t_{[16]} > 4.30$, all $p_{corr} < .001$; Fig. 2B). No significant difference was observed between both CO_2-containing conditions (CS+_US vs. US, all $t_{[16]} < 2.39$, all $p_{corr} = .157$) and both olfactory conditions (CS+ vs. CS−, all $t_{[16]} < 0.37$, all $p_{corr} > .999$). A main effect of session was found for %SCR ($F_{[1,16]} = 12.00$, $p = .003$) and Amp ($F_{[1,16]} = 7.42$, $p = .015$), but not for nSCR ($F_{[1,16]} = 3.59$, $p = 0.76$), with more pronounced SCRs in the first compared to the second session (%SCR: $t_{[16]} = 3.46$, $p_{corr} = .003$; $t_{[16]} = 2.72$, $p_{corr} = .015$). Averaged waveforms of event-related SCR responses are depicted in Fig. 2B. All mean values are reported in Table S3.

Post-scanning questionnaire

After scanning, overall CO_2 aversiveness was rated as 6.9 (±0.9, on a scale from 1 [“not perceivable”] to 9 [“too painful”], with 5 = “moderately painful”). Odor intensity was rated as 5.7 (±1.6, on a scale from 1 [“not perceivable”] to 9 [“too intense”], with 5 = “well perceivable”). Both ratings suggest that stimuli were perceived appropriately, as CS were well discernible, and the US was sufficiently aversive. When asked for describing a systematic relationship between odors and CO_2, n = 21 subjects indicated that they did not detect any relationship. One subject indicated that odors were presented to the right nostril, whereas CO_2 was presented to the left nostril. N = 6 subjects stated that CO_2 was often given “simultaneously” or “closely with” the odors. Only one subject detected that “CO_2 was more likely to be presented following the more pleasant odor” (which was vanillin in that case). Crucially, none of the other subjects became aware of the fact that only one odor was paired with the CO_2.

fMRI

Whole brain random effects analysis (T tests masked by interaction term)— During the first session, only one cluster in the right middle temporal pole showed a session-specific differential response to both CS conditions, with increased response to CS− compared to CS+ trials (CS− > CS+). During the second session, in contrast, extended suprathreshold activation could be found for the comparison CS+ > CS− in various brain regions, including mid- and mediodorsal prefrontal cortex (PFC), premotor and supplementary motor area (SMA), middle and posterior cingulate cortices, precuneus and superior parietal lobule, supramarginal and right angular gyrus, superior and middle temporal gyrus, left temporal pole, lingual gyrus and adjacent visual processing areas, the right frontal operculum extending into the inferior orbitofrontal cortex (OFC), as well as medio-dorsal and ventro-lateral nucleus of the thalamus (Fig. 3). No suprathreshold voxel appeared in the reverse contrast (CS− > CS+) in the second session. See Table 1 for a detailed overview.

ROI analyses—A significant interaction was found for the left and right amygdala (left: $F_{[1,28]} = 6.730$, $p = .015$, right: $F_{[1,28]} = 6.246$, $p = .019$) and the right POC ($F[_{1,28]} = 7.606$, $p = .010$), but not for the left POC ($F_{[1,28]} = 3.949$, $p = .057$). Post-hoc *t*-tests revealed significant differentiation between both CS conditions in the second session, with increased signal change in response to CS+ compared to CS− in the left amygdala ($t_{[28]} = 2.820$, $p_{corr} = .036$) and right POC ($t_{[28]} = 2.854$, $p_{corr} = .013$). Differential activation in the right amygdala did not survive correction for multiple comparisons ($t_{[28]} = 2.085$, $p_{uncorr} = .046$, $p_{corr} = .171$). A significant signal increase towards the CS+ condition from session 1 to session 2 could additionally be found in the right POC ($t_{[28]} = 3.051$, $p_{corr} = .020$; Fig. 3). Mean values are reported in Table S4.

Psychophysiological interaction—The comparison of *task-independent* connectivity of the aMCC between sessions revealed increased co-activation of a wide-spread network during the first session (Fig. 4), including bilateral medial and lateral prefrontal regions (such as the medial frontal gyrus, inferior, middle and superior OFC), bilateral posterior cingulate cortex, reaching into the precuneus, left middle temporal gyrus, and left angular gyrus. No significant cluster emerged in the reversed contrast (sess2 > sess1; Table 2). Analysis of *task-dependent* connectivity of the aMCC across sessions revealed a contrary picture (Table 2, Fig. 4). While no cluster showed differential connectivity during the first session, CS+-specific co-activation during the second session could be observed in the right middle and anterior insula, right sensorimotor cortex, including precentral gyrus and SMA, and right cerebellum. No cluster was found to be preferentially connected to the aMCC in CS− trials.

Discussion

The current study aimed at investigating the neural correlates of chemosensory Pavlovian conditioning, and at relating observed effects to the process of salience attribution and adaptive control. While no differential response to CS+ and CS− could be found at the behavioral and electrophysiological levels, a robust differential response to the CS+ emerged on a neural level, including frontal, temporal, occipito-parietal and subcortical brain regions. Additional ROI analyses revealed a significant impact of aversive conditioning on the primary olfactory cortex and the amygdala. By means of functional connectivity analysis, the network dynamics related to salience attribution and adaptive control were investigated as a function of conditioning, using aMCC as seed region. The connectivity profile of the aMCC reveals a strengthening of CS+-specific coupling with the right insula, sensorimotor cortex and cerebellum, which are the main input and output structures of the aMCC for exerting adaptive control. In contrast, task-unspecific connectivity throughout the brain decreased, implying a sharpening of the aMCC connectivity profile as a result of conditioning.

Pavlovian conditioning within the chemosensory system

Using a differential olfactory-trigeminal conditioning paradigm, we could demonstrate the emergence of a robust differential cerebral response to the olfactory CS+ which is suggestive of successful conditioning. While no difference in CS induced activation was evident during the first session (except for a small cluster in the middle temporal pole), a CS

+-specific increase of activation led to a significant differentiation of CS+ and CS− in a large-scale network in the second session. These brain regions included bilateral mid-and medio-dorsal PFC, sensorimotor and cingulate cortices, superior and inferior parietal lobules, temporal and occipital areas, right frontal operculum and inferior OFC, as well as the bilateral thalamus, all of which have been reported in other studies on aversive conditioning with varying consistency (for review, see Mechias et al., 2010; Sehlmeyer et al., 2009), but also in studies on pain (Iannetti and Mouraux, 2010) and emotion (Kober et al., 2008). In particular, activation of the dACC/aMCC constitutes one of the most consistent findings in aversive conditioning (Mechias et al., 2010). Our results imply that this finding can now be extended to the chemosensory modality as well. Additional ROI analyses revealed significant modulation of activation in the left amygdala and right POC, thereby replicating another well-known effect of aversive conditioning. The latter finding parallels reports of enhanced activation of primary sensory cortices in response to auditory and visual CS (e.g. Dunsmoor et al., 2007; Klucken et al., 2009). This phenomenon is mainly interpreted as modality-specific tuning of the sensory cortex as a result of conditioning, which allows enhanced encoding of the emotionally and motivationally significant stimulus (Weinberger, 2004). Consistent with this, recent studies on chemosensory event-related potentials (ERP) have shown a modulation of ERP components as early as the N1 by pain expectancy, supporting an effect of salience on the very first sensory processing levels (Bulsing et al., 2007, 2010). In our study, the differential response was more pronounced in the right POC, which might result from the right-sided olfactory stimulation and subsequent ipsilateral projections into the POC (Gottfried, 2006). The primary olfactory cortex is also discussed as a chemosensory integration area (Albrecht et al., 2010; Lundstrom et al., 2011), which might support the formation of olfactory-trigeminal associations during aversive conditioning.

With regard to the amygdala, a similar response pattern was found, however against the background of a general de-activation in response to both CS. This deactivation can be explained by the fact that ‘percent signal change’ takes the pre-stimulus activation level into account. Closer inspection of amygdala activation revealed a significant signal increase in response to the preceding attention cue, which resulted in a relative decrease of CS induced activation in the ROI analysis (see Supplementary material, Fig. S2). This activation pattern of the amygdala is consistent with numerous studies that showed heighted activation in response to ambiguity, especially in anticipation of a potential thread (Hsu et al., 2005). Our subjects largely remained contingency-unaware and might thus have reacted to the attention cue with heightened arousal in anticipation of the aversive event. The additional development of a differential amygdala response suggests that the CS+ has undergone a change in stimulus characteristics as a result of repeated pairing with the US. According to a recent meta-analysis on amygdala activation (Cunningham and Brosch, 2012), and also consistent with our hypothesis of salience attribution, this change could reflect increased emotional stimulus relevance of the CS+ which successively became a predictor of the US. Conversely, CS− induced activation tended to decrease as a result of reduced association with threat. Finally, although the lateralization of the amygdala is still a matter of debate (for review, see Baas et al., 2004; Costafreda et al., 2008), the involvement of the left amygdala in the present study is consistent with the recent finding that the left superior amygdala

showed strongest co-activation with frontal regions which were identified in a central network for emotion processing (Kober et al., 2008; Wager et al., 2003).

The present results therefore suggest that aversive conditioning within the cerebral chemosensory system is possible, with substantial resemblance to neural correlates of aversive conditioning in other modalities. Despite a general high variability of structures reported in classical conditioning studies, which is attributed to methodological differences as well as generally weak effects (Mechias et al., 2010), the combined interpretation implies a common, modality-unspecific mechanism underlying emotional learning and salience processing (as discussed below).

Dissociation of neural, electrodermal and behavioral responses in aversive conditioning

Although a robust differential response to CS+ and CS− could be found on the neural level, this was not the case for electrodermal and behavioral reactions. This stands in sharp contrast to US-containing trials, which constantly elicited a significant increase in electrodermal response, as well as reduced valence and increased intensity ratings, thereby confirming sufficient aversiveness of the trigeminal stimulus. The dissociation of neural, autonomous and behavioral conditioning effects was systematically studied in a series of fMRI experiments (Klucken et al., 2009; Tabbert et al., 2006, 2011). These could demonstrate that all subjects showed conditioning effects on the neural level, while effects on electrodermal response and valence ratings were only found in contingency-aware subjects. Contingency awareness describes the ability to verbalize the relationship between CS and US, and has been discussed as a prerequisite for autonomous and evaluative conditioning, dating back as early as 1937 (Hilgard et al., 1937). Although this topic is still a matter of debate, the majority of studies support this hypothesis (for review, see Lovibond and Shanks, 2002). Of special interest is one study using olfactory CS and a painful shock as US in which conditioned SCRs were only observed in aware subjects, and only after the onset of awareness of the CS+_US contingency (Marinkovic et al., 1989). In the present study, all subjects except for one were not able to verbalize the systematic association between odors and CO_2, suggesting that our sample was largely contingency-unaware, which in turn explains the lack of conditioning effects on autonomous and behavioral measures. One can speculate that prolonged exposure to the conditioning procedure might have fostered contingency awareness, resulting in significant responses to the CS+ in behavior and electrodermal activity. The use of a fairly low intermittent coupling rate of 60% (Leonard, 1975), as well as olfactory habituation, which leads to a progressive degradation of the olfactory percept (Dalton, 2000), might have slowed the emergence of contingency awareness. In addition, the use of interspersed US trials reduced the predictive value (or “information” according to Rescorla, 1988) of the CS+, which may have resulted in a slowing of the conditioning process. Another aspect which might have counteracted conditioning is the fact that both odors were rated as mildly pleasant, and it is known that positively valenced CS are more difficult to be conditioned to an aversive US. This procedure, also known as counter-conditioning (Bouton, 2004), is associated with slower development of a conditioned response (Nasser and McNally, 2012). Finally, the sense of smell primarily acts beyond consciousness (Koster et al., 2002), presumably due to its unique anatomical (i.e. no thalamic intermediary; Carmichael et al., 1994; Gottfried, 2006)

and physiological (i.e. rapid central and peripheral sensory adaptation; Best and Wilson, 2004) properties. This particularity of the sense of smell might pose additional constraints on the acquisition of contingency awareness for odors.

Conditioned brain activation as an adaptive control response

When comparing CS-induced brain activation in the second session, most pronounced effects were found in a cluster involving the middle frontal gyrus, extending laterally into the DLPFC, and medially into the dorsomedial superior frontal gyrus, aMCC, pMCC, and SMA. This cluster can be best interpreted in the context of executive function and motor control in the face of perceived salience. Recent findings on connectivity patterns and behavioral–functional profiles of the cingulate cortex imply a successive integration of salience and adaptive motor control along an anterior-to-posterior axis, which might culminate in the execution of a motor response (Beckmann et al., 2009; Torta and Cauda, 2011). A first integration might take place in the anterior portion of the MCC, the aMCC, which has already been introduced as key node of the salience network (see Introduction). While the ventral portion of the aMCC has been shown to be preferentially connected with structures of the ventral attentional system implicated in emotion and salience detection, the dorsal portion shows stronger connectivity with structures associated with the dorsal attentional system involved in goal-directed behavior and executive function (Beckmann et al., 2009; Torta and Cauda, 2011). The integrative function of the MCC in dedication to salience-guided motor control is also reflected in the so-called cingulate zones, which have first been described in the macaque as somatotopically organized premotor areas and are assumed to exist in humans as well (Picard and Strick, 2001). While the rostral cingulate zone (RCZ) in the aMCC relates to more cognitive and motivational aspects of action control (e.g. reinforcement-guided action selection), the caudal cingulate zone (CCZ) in the pMCC is implicated in rather basic aspects of movement control and spatial attention (Picard and Strick, 2001; Shackman et al., 2011). Interestingly, while the observed response of the MCC suggests the activation of all three cingulate zones, the location of our aMCC seed region, deep within the cingulate sulcus, seems to specifically coincide with the anterior RCZ. Taken together, our finding of a joint activation of the entire MCC with instances of the ventral attentional system (e.g. right frontal operculum and inferior OFC, bilateral mediodorsal thalamus), dorsal attentional system (e.g. bilateral dorsal PFC and superior parietal cortices) and motor system (e.g. bilateral SMA, left premotor area) suggests that subjects learned to mobilize the adaptive control system upon detection of the CS+ in anticipation of the painful US. This is consistent with other studies on aversive conditioning and pain discrimination, which repeatedly reported activation of the dACC/aMCC and SMA, independent of whether motor responses were included in the paradigm or not (Oertel et al., 2012; Peyron et al., 2000; Spoormaker et al., 2011; Tabbert et al., 2005). Referring to motor responses, it is very likely that the instrumental response in our study, in which subjects had to press a button in order to avoid an increase of US intensity, added to the motor-related activity in response to the CS+. Subjects might have prepared to press the button upon CS+ detection as a result of conditioning, which, however, can be regarded as another instance of the adaptive control response to the CS+. This interpretation is partly supported by the improvement of response times in the second session, which tended to be more pronounced for the CS+_US compared to the US-only condition.

Functional connectivity of the aMCC during chemosensory Pavlovian conditioning

The idea of the aMCC/dACC as part of the salience network is based on studies using various experimental approaches, such as task-based fMRI (Downar et al., 2003; Drabant et al., 2011; Mouraux et al., 2011), resting state functional connectivity fMRI (Cauda et al., 2011; Seeley et al., 2007; Taylor et al., 2009), and psychophysiological interaction (Wiech et al., 2010). In our study, the development of a preferential CS+-specific connectivity of the right aMCC with the right central and anterior insula, sensorimotor cortex, and cerebellum in the second half of the experiment is in favor of this network hypothesis. No enhanced task-dependent connectivity of the aMCC with any other brain region was found in the CS− condition, and in both CS conditions during the first session. In contrast, task-*independent* connectivity of the aMCC decreased from session 1 to session 2. While significant coupling with the aMCC was observed in mediofrontal brain regions, PCC, precuneus, left angular and middle temporal gyrus during the first session, no brain region showed task-independent connectivity with aMCC during the second session. These data imply a sharpening of the connectivity profile of the aMCC, which was unspecific at the beginning of the conditioning task and rather related to the default mode network (Greicius et al., 2003), but gained specificity during the course of the experiment, with AI as putative input structure, and sensorimotor areas as putative output structure in the context of salience processing and adaptive control. In accordance with this hypothesis, activity of the salience network, and more specifically of the right AI, has been shown to entrain activity in other brain regions (Sridharan et al., 2008), which finally leads to a network switch from an internally oriented default mode (i.e. default mode network) to an externally oriented mode of executive control for efficient operation on the identified salience (i.e. executive control network; Menon and Uddin, 2010; Seeley et al., 2007). The right-sided lateralization of brain regions showing task-dependent connectivity likely results from the localization of our aMCC seed region within the right hemisphere. Independent of anatomical connectivity, previous studies suggest a right-sided dominance for salience processing in the AI (Craig, 2009; Eckert et al., 2009). Another finding with relevance for the present results is the AI's involvement in the coding of prediction errors with respect to subjective feeling states and risk (Singer et al., 2009), which is reflected in Damasio's well-known somatic marker hypothesis (Damasio, 1994). Prediction error coding represents a major theoretical framework of Pavlovian conditioning (Ludvig et al., 2012), and has been shown to apply to the AI as well (d'Acremont et al., 2009; Seymour et al., 2004). The increased connectivity between the AI and aMCC implies that a risk prediction error was generated in the AI upon detection of the CS+, which in turn entrained activation of the adaptive control system.

Finally, the CS+-specific connectivity of the aMCC included a cluster in the right cerebellum which was situated in lobule VI and extended crus I and lobule VIIa. The involvement of the cerebellum, especially of the phylogenetically younger lobules VI–VII (Kelly and Strick, 2003), in non-motor functions has repeatedly been shown (for review, see Stoodley, 2012). A recent connectivity study identified distinct, largely non-overlapping regions within the cerebellum which contribute to intrinsic connectivity networks of the brain (Habas et al., 2009). In line with our hypothesis of salience attribution and adaptive control, the cerebellar activation observed in the present study almost perfectly overlaps with the portion of the cerebellum which was identified as part of the salience network.

Habas and colleagues propose that lobule VI–crus I might be involved in the modulation of subcortical structures involved in salience processing. Interestingly, the authors could also show that the only overlap of networks within the cerebellum was found between the salience and sensorimotor network, suggesting a complementary link of salience detection and limbic motor control on the cerebellar level. Adding to these findings, the present results suggest that the cerebellum contributes to complex salience mechanisms, which might include the preferential allocation of arousal or alertness to instances of the salience network, or even the attribution of salience and adaptive response selection. From a clinical perspective, this might be of relevance in view of diagnosis and therapeutic interventions after cerebellar lesions, given that a disruption of the salience network should result in a wide array of cognitive deficits (e.g. attention and flexibility, emotion and motivation, executive functions), which are indeed often found after cerebellar stroke (e.g. the cerebellar cognitive affective syndrome, CCAS; Schmahmann and Sherman, 1998; for review, see Stoodley and Schmahmann, 2010).

Limitations and outlook

One limitation of the present study is the assessment of contingency awareness by means of self-report without an additional standardized multiple-choice questionnaire or rating task (Klucken et al., 2009; Lovibond and Shanks, 2002). Free recall is less sensitive than recognition tests (Dawson and Reardon, 1973), which might have limited the sensitivity of our awareness measure. However, subjects were instructed to mention anything that came to their mind regarding the relationship of odors and CO_2. There was no time pressure, and an impact of forgetting or interference was minimized by assessing contingency awareness immediately following the conditioning experiment. We explicitly refrained from using a continuous expectancy measure during the experiment, as this measurement approach directly affects contingency awareness by drawing the attention to contingencies, and is therefore questionable in terms of validity (Lovibond and Shanks, 2002).

Another limitation is the use of interspersed US trials (necessary in the context of fMRI) which reduces the predictive value of the CS+ due to decreased contingency (Rescorla, 1988). Using an intermittent reinforcement schedule with reduced contiguity, the predictive value of CS+ was further lowered. However, the probability of $p(US| CS+) = 0.57$ was still substantially greater than the probability $p(US| \sim CS+)$, which is 0.25. Altogether, the current reinforcement schedule should allow for sufficient contingency and contiguity between US and CS+, though conditioning might evolve rather slowly and might not have been completed by the end of session 2. These circumstances might contribute to the present findings of a differential response on the neural, but not on the behavioral and electrodermal level.

Finally, the absence of behavioral and electrodermal conditioning effects does not allow a clear-cut interpretation of the results. In order to acknowledge the differential response on the neural level as a result of aversive conditioning, it should at best be linked to differential effects in behavior and/or electrophysiology. Although the lack of contingency awareness offers an explanation for the present findings, the introduction of a second, contingency-

aware group would be desirable to unequivocally interpret brain activation in the context of conditioning in future studies.

Adding to this, it would be of clinical interest to apply chemosensory conditioning for testing certain neurodegenerative diseases given the fact that olfactory deficits are amongst the most precocious signs heralding Parkinson's disease, Huntington's disease, and other neurodegenerative conditions (Ruan et al., 2012).

Conclusions

In conclusion, the present findings suggest that Pavlovian aversive conditioning is a suitable approach for characterizing the dynamics of salience attribution and adaptive control. Repeated coupling of a previously neutral CS with a noxious US led to enhanced connectivity of the aMCC with regions implicated in salience detection and effective motor control. These changes were paralleled by the emergence of differential, large-scale network activation in response to the CS+, thereby demonstrating substantial similarities of conditioning within the chemosensory and other sensory systems. The independence from effects on the behavioral and autonomous level implies that changes on the neural level do not instantaneously result in the effective generation of adaptive responses. The transition from a neural-only to a multilevel response might be a function of contingency awareness.

Supplementary Material

Refer to Web version on PubMed Central for supplementary material.

Acknowledgments

The authors would like to thank Frank Boers for providing a computer interface for controlling the olfactometer, as well as Christina Regenbogen for helpful support during data analysis.

Funding

This work was supported by the German Research Foundation (DFG, IRTG 1328) and the Interdisciplinary Centre for Clinical Research of the Medical Faculty of the RWTH Aachen University (IZKF, N4-4).

References

Albrecht J, Kopietz R, Frasnelli J, Wiesmann M, Hummel T, Lundstrom JN. The neuronal correlates of intranasal trigeminal function—an ALE meta-analysis of human functional brain imaging data. Brain Res Rev. 2010; 62:183–196. [PubMed: 19913573]

Ashburner J, Friston KJ. Unified segmentation. NeuroImage. 2005; 26:839–851. [PubMed: 15955494]

Baas D, Aleman A, Kahn RS. Lateralization of amygdala activation: a systematic review of functional neuroimaging studies. Brain Res Rev. 2004; 45:96–103. [PubMed: 15145620]

Beckmann M, Johansen-Berg H, Rushworth MF. Connectivity-based parcellation of human cingulate cortex and its relation to functional specialization. J Neurosci. 2009; 29:1175–1190. [PubMed: 19176826]

Benedek M, Kaernbach C. Decomposition of skin conductance data by means of nonnegative deconvolution. Psychophysiology. 2010; 47:647–658. [PubMed: 20230512]

Bensafi M, Frasnelli J, Reden J, Hummel T. The neural representation of odor is modulated by the presence of a trigeminal stimulus during odor encoding. Clin Neurophysiol. 2007; 118:696–701. [PubMed: 17208517]

Best AR, Wilson DA. Coordinate synaptic mechanisms contributing to olfactory cortical adaptation. J Neurosci. 2004; 24:652–660. [PubMed: 14736851]

Bouton ME. Context and behavioral processes in extinction. Learn Mem. 2004; 11:485–494. [PubMed: 15466298]

Büchel C, Dolan RJ, Armony JL, Friston KJ. Amygdala-hippocampal involvement in human aversive trace conditioning revealed through event-related functional magnetic resonance imaging. J Neurosci. 1999; 19:10869–10876. [PubMed: 10594068]

Bulsing PJ, Smeets MA, Hummel T, van den Hout MA. Influence of chemosensory pain-expectancy on olfactory event-related potentials. NeuroImage. 2007; 38:164–170. [PubMed: 17728154]

Bulsing PJ, Smeets MA, Gemeinhardt C, Laverman M, Schuster B, Van den Hout MA, Hummel T. Irritancy expectancy alters odor perception: evidence from olfactory event-related potential research. J Neurophysiol. 2010; 104:2749–2756. [PubMed: 20844114]

Busch CJ, Evans IM. The effectiveness of electric shock and foul odor as unconditioned stimuli in classical aversive conditioning. Behav Res Ther. 1977; 15:167–175. [PubMed: 869866]

Carmichael ST, Clugnet MC, Price JL. Central olfactory connections in the macaque monkey. J Comp Neurol. 1994; 346:403–434. [PubMed: 7527806]

Caspers S, Geyer S, Schleicher A, Mohlberg H, Amunts K, Zilles K. The human inferior parietal cortex: cytoarchitectonic parcellation and interindividual variability. NeuroImage. 2006; 33:430–448. [PubMed: 16949304]

Cauda F, D'Agata F, Sacco K, Duca S, Geminiani G, Vercelli A. Functional connectivity of the insula in the resting brain. NeuroImage. 2011; 55:8–23. [PubMed: 21111053]

Choi HJ, Zilles K, Mohlberg H, Schleicher A, Fink GR, Armstrong E, Amunts K. Cytoarchitectonic identification and probabilistic mapping of two distinct areas within the anterior ventral bank of the human intraparietal sulcus. J Comp Neurol. 2006; 495:53–69. [PubMed: 16432904]

Costafreda SG, Brammer MJ, David AS, Fu CH. Predictors of amygdala activation during the processing of emotional stimuli: a meta-analysis of 385 PET and fMRI studies. Brain Res Rev. 2008; 58:57–70. [PubMed: 18076995]

Craig AD. How do you feel—now? The anterior insula and human awareness. Nat Rev Neurosci. 2009; 10:59–70. [PubMed: 19096369]

Cunningham WA, Brosch T. Motivational salience: amygdala tuning from traits, needs, values, and goals. Curr Dir Psychol Sci. 2012; 21:45–59.

d'Acremont M, Lu ZL, Li X, Van der Linden M, Bechara A. Neural correlates of risk prediction error during reinforcement learning in humans. NeuroImage. 2009; 47:1929–1939. [PubMed: 19442744]

Dalton P. Psychophysical and behavioral characteristics of olfactory adaptation. Chem Senses. 2000; 25:487–492. [PubMed: 10944515]

Damasio AR. Descartes' error and the future of human life. Sci Am. 1994; 271:144. [PubMed: 7939563]

Dawson ME, Reardon P. Construct validity of recall and recognition postconditioning measures of awareness. J Exp Psychol. 1973; 98:308–315. [PubMed: 4705630]

Diedrichsen J, Balsters JH, Flavell J, Cussans E, Ramnani N. A probabilistic MR atlas of the human cerebellum. NeuroImage. 2009; 46:39–46. [PubMed: 19457380]

Doty RL, Brugger WE, Jurs PC, Orndorff MA, Snyder PJ, Lowry LD. Intranasal trigeminal stimulation from odorous volatiles: psychometric responses from anosmic and normal humans. Physiol Behav. 1978; 20:175–185. [PubMed: 662939]

Downar J, Mikulis DJ, Davis KD. Neural correlates of the prolonged salience of painful stimulation. NeuroImage. 2003; 20:1540–1551. [PubMed: 14642466]

Drabant EM, Kuo JR, Ramel W, Blechert J, Edge MD, Cooper JR, Goldin PR, Hariri AR, Gross JJ. Experiential, autonomic, and neural responses during threat anticipation vary as a function of threat intensity and neuroticism. NeuroImage. 2011; 55:401–410. [PubMed: 21093595]

Dunsmoor JE, Bandettini PA, Knight DC. Impact of continuous versus intermittent CS−UCS pairing on human brain activation during Pavlovian fear conditioning.Behav. Neurosci. 2007; 121:635–642.

Eckert MA, Menon M, Walczac A, Ahlstrom J, Denslow S, Horwitz A, Dubno JR. At the heart of the ventral attentional system: the right anterior insula. Hum Brain Mapp. 2009; 30:2530–2541. [PubMed: 19072895]

Eickhoff SB, Heim S, Zilles K, Amunts K. Testing anatomically specified hypotheses in functional imaging using cytoarchitectonic maps. NeuroImage. 2006a; 32:570–582. [PubMed: 16781166]

Eickhoff SB, Schleicher A, Zilles K, Amunts K. The human parietal operculum. I.Cytoarchitectonic mapping of subdivisions. Cereb Cortex. 2006b; 16:254–267. [PubMed: 15888607]

Farrell MJ, Laird AR, Egan GF. Brain activity associated with painfully hot stimuli applied to the upper limb: a meta-analysis. Hum Brain Mapp. 2005; 25:129–139. [PubMed: 15846813]

Frasnelli J, Hummel T, Berg J, Huang G, Doty RL. Intranasal localizability of odorants: influence of stimulus volume. Chem Senses. 2011; 36:405–410. [PubMed: 21310764]

Geyer S. The microstructural border between the motor and the cognitive domain in the human cerebral cortex. Adv Anat Embryol Cell Biol. 2004; 174(I–VIII):1–89.

Geyer S, Ledberg A, Schleicher A, Kinomura S, Schormann T, Burgel U, Klingberg T, Larsson J, Zilles K, Roland PE. Two different areas within the primary motor cortex of man. Nature. 1996; 382:805–807. [PubMed: 8752272]

Geyer S, Schleicher A, Zilles K. Areas 3a, 3b, and 1 of human primary somatosensory cortex. NeuroImage. 1999; 10:63–83. [PubMed: 10385582]

Gottfried JA. Smell: central nervous processing. Adv Otorhinolaryngol. 2006; 63:44–69. [PubMed: 16733332]

Gottfried JA, O'Doherty J, Dolan RJ. Appetitive and aversive olfactory learning in humans studied using event-related functional magnetic resonance imaging. J Neurosci. 2002; 22:10829–10837. [PubMed: 12486176]

Grefkes C, Geyer S, Schormann T, Roland P, Zilles K. Human somatosensory area 2: observer-independent cytoarchitectonic mapping, interindividual variability, and population map. NeuroImage. 2001; 14:617–631. [PubMed: 11506535]

Greicius MD, Krasnow B, Reiss AL, Menon V. Functional connectivity in the resting brain: a network analysis of the default mode hypothesis. Proc Natl Acad Sci U S A. 2003; 100:253–258. [PubMed: 12506194]

Habas C, Kamdar N, Nguyen D, Prater K, Beckmann CF, Menon V, Greicius MD. Distinct cerebellar contributions to intrinsic connectivity networks. J Neurosci. 2009; 29:8586–8594. [PubMed: 19571149]

Hautzinger M, Keller F, Kühner C. Beck Depressions-Inventar (BDI-II). Harcourt Test Services, Frankfurt/Main (Revision). 2006

Heinz A, Schlagenhauf F. Dopaminergic dysfunction in schizophrenia: salience attribution revisited. Schizophr Bull. 2010; 36:472–485. [PubMed: 20453041]

Hermann C, Ziegler S, Birbaumer N, Flor H. Pavlovian aversive and appetitive odor conditioning in humans: subjective, peripheral, and electrocortical changes. Exp Brain Res. 2000; 132:203–215. [PubMed: 10853945]

Hilgard ER, Campbell RK, Sears WN. Conditioned discrimination: the effect of knowledge of stimulus relationships. Am J Psychol. 1937; 51:498–506.

Hsu M, Bhatt M, Adolphs R, Tranel D, Camerer CF. Neural systems responding to degrees of uncertainty in human decision-making. Science. 2005; 310:1680–1683. [PubMed: 16339445]

Hummel T, Konnerth CG, Rosenheim K, Kobal G. Screening of olfactory function with a four-minute odor identification test: reliability, normative data, and investigations in patients with olfactory loss. Ann Otol Rhinol Laryngol. 2001; 110:976–981. [PubMed: 11642433]

Iannetti GD, Mouraux A. From the neuromatrix to the pain matrix (and back). Exp Brain Res. 2010; 205:1–12. [PubMed: 20607220]

Jensen J, Willeit M, Zipursky RB, Savina I, Smith AJ, Menon M, Crawley AP, Kapur S. The formation of abnormal associations in schizophrenia: neural and behavioral evidence. Neuropsychopharmacology. 2008; 33:473–479. [PubMed: 17473838]

Kelly RM, Strick PL. Cerebellar loops with motor cortex and prefrontal cortex of a nonhuman primate. J Neurosci. 2003; 23:8432–8444. [PubMed: 12968006]

Klucken T, Kagerer S, Schweckendiek J, Tabbert K, Vaitl D, Stark R. Neural, electrodermal and behavioral response patterns in contingency aware and unaware subjects during a picture–picture conditioning paradigm. Neuroscience. 2009; 158:721–731. [PubMed: 18976695]

Kober H, Barrett LF, Joseph J, Bliss-Moreau E, Lindquist K, Wager TD. Functional grouping and cortical–subcortical interactions in emotion: a meta-analysis of neuroimaging studies. NeuroImage. 2008; 42:998–1031. [PubMed: 18579414]

Koster EP, Degel J, Piper D. Proactive and retroactive interference in implicit odor memory. Chem Senses. 2002; 27:191–206. [PubMed: 11923182]

Leonard DW. Partial reinforcement effects in classical aversive conditioning in rabbits and human beings. J Comp Physiol Psychol. 1975; 88:596–608. [PubMed: 1150940]

Livermore A, Hummel T, Kobal G. Chemosensory event-related potentials in the investigation of interactions between the olfactory and the somatosensory (trigeminal) systems. Electroencephalogr Clin Neurophysiol. 1992; 83:201–210. [PubMed: 1381671]

Lovibond PF, Shanks DR. The role of awareness in Pavlovian conditioning: empirical evidence and theoretical implications. J Exp Psychol Anim Behav Process. 2002; 28:3–26. [PubMed: 11868231]

Ludvig EA, Sutton RS, Kehoe EJ. Evaluating the TD model of classical conditioning. Learn Behav. 2012; 40:305–319. [PubMed: 22927003]

Lundstrom JN, Boesveldt S, Albrecht J. Central processing of the chemical senses: an overview. ACS Chem Neurosci. 2011; 2:5–16. [PubMed: 21503268]

Malikovic A, Amunts K, Schleicher A, Mohlberg H, Eickhoff SB, Wilms M, Palomero-Gallagher N, Armstrong E, Zilles K. Cytoarchitectonic analysis of the human extrastriate cortex in the region of V5/MT+: a probabilistic, stereotaxic map of area hOc5. Cereb Cortex. 2007; 17:562–574. [PubMed: 16603710]

Marinkovic K, Schell AM, Dawson ME. Awareness of the CS−UCS contingency and classical conditioning of skin conductance responses with olfactory CSs. Biol Psychol. 1989; 29:39–60. [PubMed: 2590708]

Mechias ML, Etkin A, Kalisch R. A meta-analysis of instructed fear studies: implications for conscious appraisal of threat. NeuroImage. 2010; 49:1760–1768. [PubMed: 19786103]

Menon V, Uddin LQ. Saliency, switching, attention and control: a network model of insula function. Brain Struct Funct. 2010; 214:655–667. [PubMed: 20512370]

Moessnang C, Habel U, Schneider F, Siegel SJ. The electrophysiological signature of motivational salience in mice and implications for schizophrenia. Neuropsychopharmacology. 2012; 37:2846–2854. [PubMed: 22910459]

Morris JS, Büchel C, Dolan RJ. Parallel neural responses in amygdala subregions and sensory cortex during implicit fear conditioning. NeuroImage. 2001; 13:1044–1052. [PubMed: 11352610]

Mouraux A, Diukova A, Lee MC, Wise RG, Iannetti GD. A multisensory investigation of the functional significance of the “pain matrix”. NeuroImage. 2011; 54:2237–2249. [PubMed: 20932917]

Nasser HM, McNally GP. Appetitive-aversive interactions in Pavlovian fear conditioning. Behav Neurosci. 2012; 126:404–422. [PubMed: 22642885]

Oertel BG, Preibisch C, Martin T, Walter C, Gamer M, Deichmann R, Lotsch J. Separating brain processing of pain from that of stimulus intensity. Hum Brain Mapp. 2012; 33:883–894. [PubMed: 21681856]

Oldfield RC. The assessment and analysis of handedness: the Edinburgh Inventory. Neuropsychologia. 1971; 9:97–113. [PubMed: 5146491]

O’Reilly JX, Woolrich MW, Behrens TE, Smith SM, Johansen-Berg H. Tools of the trade: psychophysiological interactions and functional connectivity. Soc Cogn Affect Neurosci. 2012; 7:604–609. [PubMed: 22569188]

Peyron R, Laurent B, Garcia-Larrea L. Functional imaging of brain responses to pain. A review and meta-analysis (2000). Neurophysiol Clin. 2000; 30:263–288. [PubMed: 11126640]

Picard N, Strick PL. Imaging the premotor areas. Curr Opin Neurobiol. 2001; 11:663–672. [PubMed: 11741015]

Rescorla RA. Behavioral studies of Pavlovian conditioning. Annu Rev Neurosci. 1988; 11:329–352. [PubMed: 3284445]

Roiser JP, Stephan KE, den Ouden HE, Barnes TR, Friston KJ, Joyce EM. Do patients with schizophrenia exhibit aberrant salience? Psychol Med. 2009; 39:199–209. [PubMed: 18588739]

Rottschy C, Eickhoff SB, Schleicher A, Mohlberg H, Kujovic M, Zilles K, Amunts K. Ventral visual cortex in humans: cytoarchitectonic mapping of two extrastriate areas. Hum Brain Mapp. 2007; 28:1045–1059. [PubMed: 17266106]

Ruan Y, Zheng XY, Zhang HL, Zhu W, Zhu J. Olfactory dysfunctions in neurodegenerative disorders. J Neurosci Res. 2012; 90:1693–1700. [PubMed: 22674288]

Scheperjans F, Hermann K, Eickhoff SB, Amunts K, Schleicher A, Zilles K. Observer-independent cytoarchitectonic mapping of the human superior parietal cortex. Cereb Cortex. 2008; 18:846–867. [PubMed: 17644831]

Schmahmann JD, Sherman JC. The cerebellar cognitive affective syndrome. Brain. 1998; 121(Pt 4): 561–579. [PubMed: 9577385]

Seeley WW, Menon V, Schatzberg AF, Keller J, Glover GH, Kenna H, Reiss AL, Greicius MD. Dissociable intrinsic connectivity networks for salience processing and executive control. J Neurosci. 2007; 27:2349–2356. [PubMed: 17329432]

Sehlmeyer C, Schoning S, Zwitserlood P, Pfleiderer B, Kircher T, Arolt V, Konrad C. Human fear conditioning and extinction in neuroimaging: a systematic review. PLoS One. 2009; 4:e5865. [PubMed: 19517024]

Seymour B, O'Doherty JP, Dayan P, Koltzenburg M, Jones AK, Dolan RJ, Friston KJ, Frackowiak RS. Temporal difference models describe higher-order learning in humans. Nature. 2004; 429:664–667. [PubMed: 15190354]

Shackman AJ, Salomons TV, Slagter HA, Fox AS, Winter JJ, Davidson RJ. The integration of negative affect, pain and cognitive control in the cingulate cortex. Nat Rev Neurosci. 2011; 12:154–167. [PubMed: 21331082]

Shepherd GM. The human sense of smell: are we better than we think? PLoS Biol. 2004; 2:e146. [PubMed: 15138509]

Singer T, Critchley HD, Preuschoff K. A common role of insula in feelings, empathy and uncertainty. Trends Cogn Sci. 2009; 13:334–340. [PubMed: 19643659]

Spoormaker VI, Andrade KC, Schroter MS, Sturm A, Goya-Maldonado R, Samann PG, Czisch M. The neural correlates of negative prediction error signaling in human fear conditioning. NeuroImage. 2011; 54:2250–2256. [PubMed: 20869454]

Sridharan D, Levitin DJ, Menon V. A critical role for the right fronto-insular cortex in switching between central-executive and default-mode networks. Proc Natl Acad Sci U S A. 2008; 105:12569–12574. [PubMed: 18723676]

Sterzer P, Kleinschmidt A. Anterior insula activations in perceptual paradigms: often observed but barely understood. Brain Struct Funct. 2010; 214:611–622. [PubMed: 20512379]

Stoodley CJ. The cerebellum and cognition: evidence from functional imaging studies. Cerebellum. 2012; 11:352–365. [PubMed: 21373864]

Stoodley CJ, Schmahmann JD. Evidence for topographic organization in the cerebellum of motor control versus cognitive and affective processing. Cortex. 2010; 46:831–844. [PubMed: 20152963]

Tabbert K, Stark R, Kirsch P, Vaitl D. Hemodynamic responses of the amygdala, the orbitofrontal cortex and the visual cortex during a fear conditioning paradigm. Int J Psychophysiol. 2005; 57:15–23. [PubMed: 15935259]

Tabbert K, Stark R, Kirsch P, Vaitl D. Dissociation of neural responses and skin conductance reactions during fear conditioning with and without awareness of stimulus contingencies. NeuroImage. 2006; 32:761–770. [PubMed: 16651009]

Tabbert K, Merz CJ, Klucken T, Schweckendiek J, Vaitl D, Wolf OT, Stark R. Influence of contingency awareness on neural, electrodermal and evaluative responses during fear conditioning. Soc Cogn Affect Neurosci. 2011; 6:495–506. [PubMed: 20693389]

Taylor KS, Seminowicz DA, Davis KD. Two systems of resting state connectivity between the insula and cingulate cortex. Hum Brain Mapp. 2009; 30:2731–2745. [PubMed: 19072897]

Todrank J, Byrnes D, Wrzniewski A, Rozin P. Odors can change preferences for people in photographs: a cross-modal evaluative conditioning study with olfactory USs and visual CSs. Learn Motiv. 1995; 26:116–140.

Torta DM, Cauda F. Different functions in the cingulate cortex, a meta-analytic connectivity modeling study. NeuroImage. 2011; 56:2157–2172. [PubMed: 21459151]

Tzourio-Mazoyer N, Landeau B, Papathanassiou D, Crivello F, Etard O, Delcroix N, Mazoyer B, Joliot M. Automated anatomical labeling of activations in SPM using macroscopic anatomical parcellation of the MNI MRI single subject brain. NeuroImage. 2002; 15:273–289. [PubMed: 11771995]

Vogt BA. Pain and emotion interactions in subregions of the cingulate gyrus. Nat Rev Neurosci. 2005; 6:533–544. [PubMed: 15995724]

Wager TD, Phan KL, Liberzon I, Taylor SF. Valence, gender, and lateralization of functional brain anatomy in emotion: a meta-analysis of findings from neuroimaging. NeuroImage. 2003; 19:513–531. [PubMed: 12880784]

Weinberger NM. Specific long-term memory traces in primary auditory cortex. Nat Rev Neurosci. 2004; 5:279–290. [PubMed: 15034553]

Wiech K, Lin CS, Brodersen KH, Bingel U, Ploner M, Tracey I. Anterior insula integrates information about salience into perceptual decisions about pain. J Neurosci. 2010; 30:16324–16331. [PubMed: 21123578]

Wittchen HU, Zaudig M, Fydrich T. SKID-I/II: Strukturiertes klinisches Interview für DSM-IV. Hogrefe, Göttingen. 1997

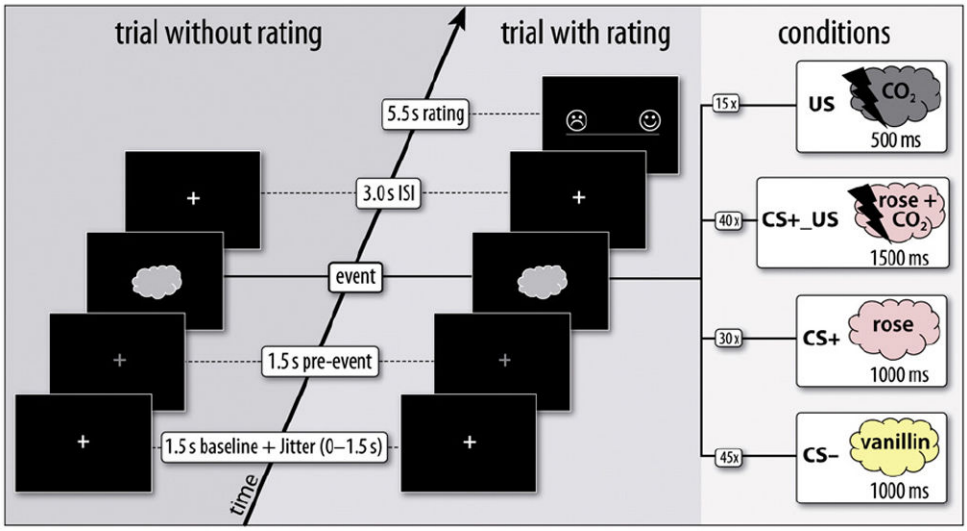

Fig. 1.

Overview of the experimental design. An exemplary trial without rating, and a trial with valence rating are depicted. Intensity ratings of the CS were illustrated as clouds of increasing shape, whereas aversiveness ratings were illustrated as flashes of increasing shape along the scale. In this example, rose is assigned to the CS+, and vanillin to the CS− condition.

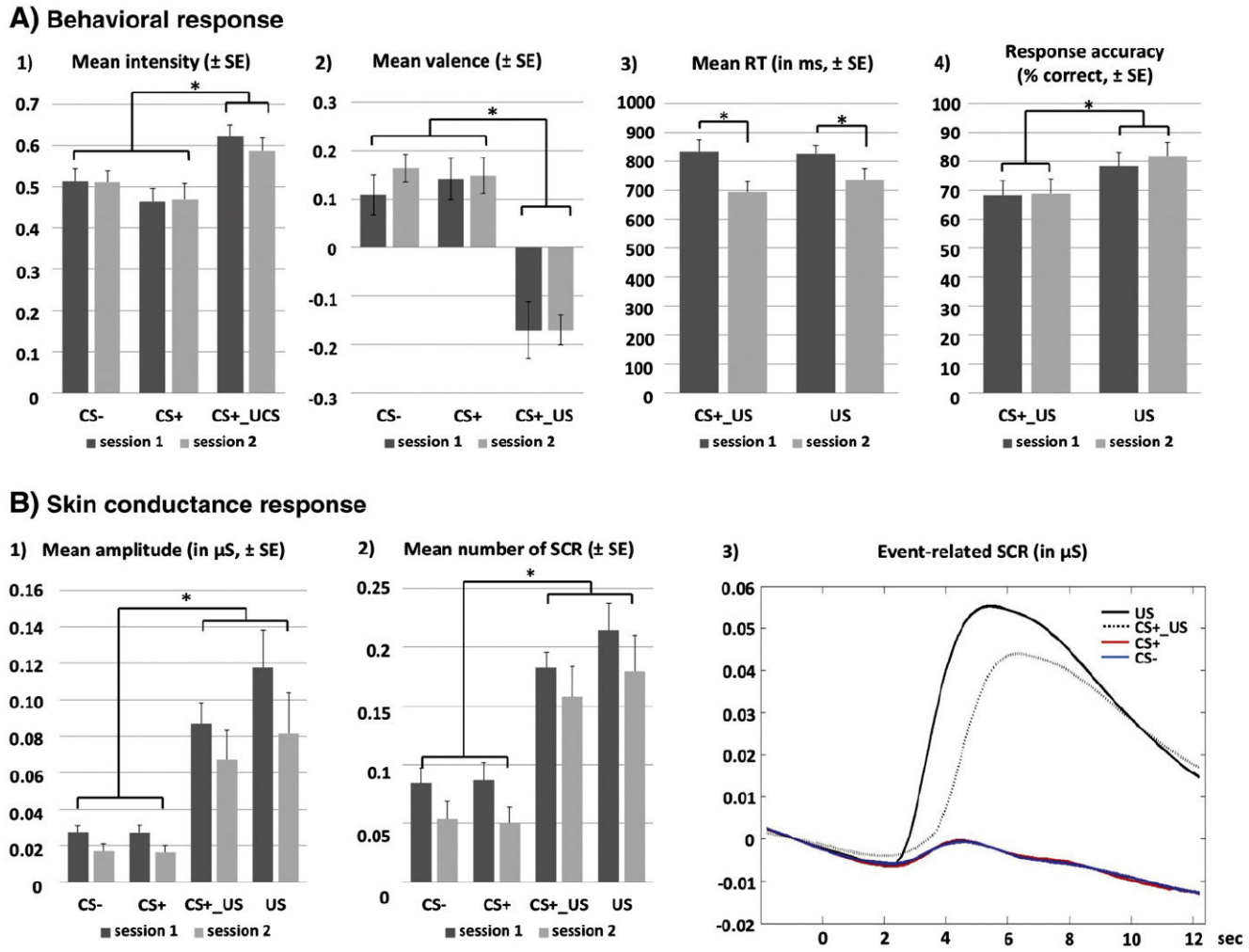

Fig. 2.

Bar graphs displaying mean behavioral performance (A) and autonomous response (B) across sessions. A main effect of condition could be found for intensity (A1) and valence ratings (A2), with higher intensity and reduced valence ratings for the bimodal CS+_US compared to pure olfactory conditions (CS−, CS+). No significant difference was found between CS+ and CS− in both sessions in either rating. Button presses in response to the US were more accurate for US-only conditions (i.e. main effect of condition, A3), whereas response times were faster in the second compared to the first session (i.e. main effect of session, A4). A main effect of condition also emerged for autonomous variables, with increased amplitude (B1) and number of skin conductance responses (SCRs, B2) in US-containing conditions (CS+_US, US), compared to only-olfactory conditions (CS+, CS−). Event-related SCR-curves are shown in B3) as condition-wise group average of the stimulus-locked time-window (−2 to 12 s). Analysis was performed in the time window from 2 to 10 s after stimulus onset. Abbreviation SE: standard error of the mean, $*p_{corr} < .05$.

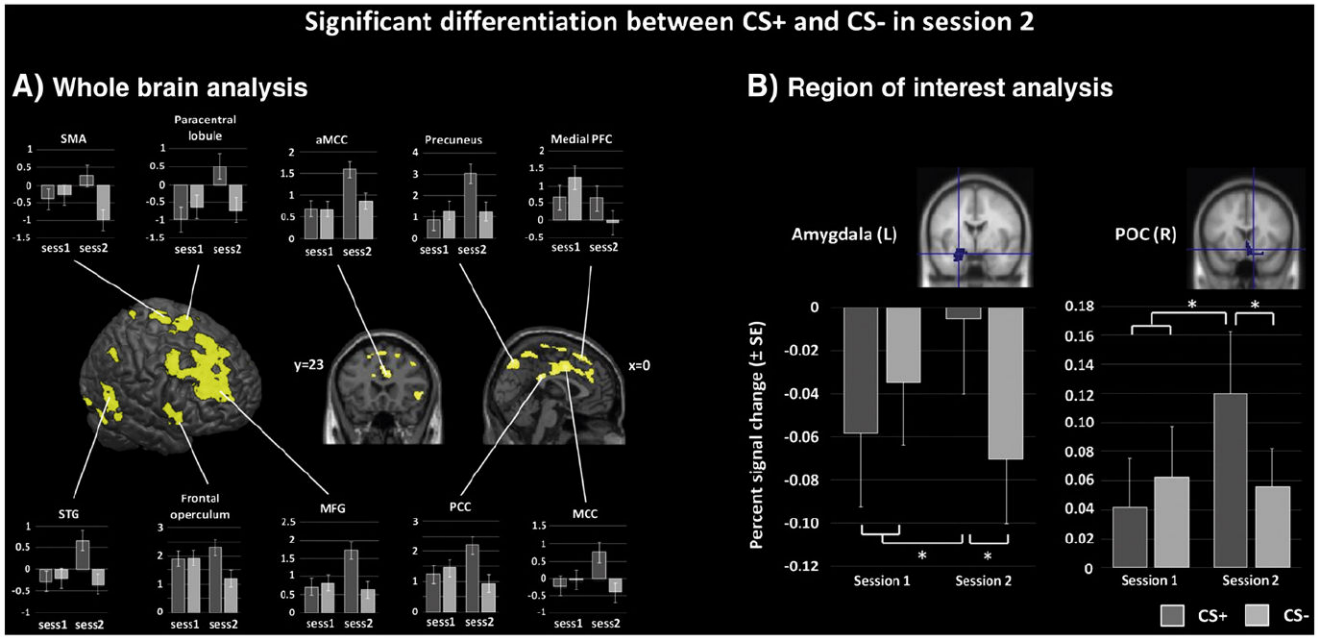

Fig. 3.

Differential BOLD effects to CS+ and CS− as a result of conditioning. A: SPM{T}-maps displaying significantly increased activation to CS+ compared to CS− during the second session. No suprathreshold voxel was observed in the reversed contrast. Bar graphs of contrast estimates (±standard error of the mean) are plotted for selected peak voxels of the corresponding cluster (paracentral lobule: [3–26 72], supplementary motor area (SMA): [−8 –5 71], medial prefrontal cortex (PFC): [3 2 54], precuneus: [2–26 72], middle cingulate cortex (MCC): [0 2 39], superior temporal gyrus (STG): [68–47 15], frontal operculum: [54 21–2], middle frontal gyrus (MFG): [29 45 32], posterior cingulate cortex (PCC): [3–36 29], anterior MCC (aMCC): [8 23 29]). x-, y-, and z-coordinates are referenced to MNI space. B: bar graphs displaying mean percent signal change (±standard error of the mean) in the left amygdala and right primary olfactory cortex (POC) in response to CS+ and CS− in the first and second session. *$p_{corr} < .05$.

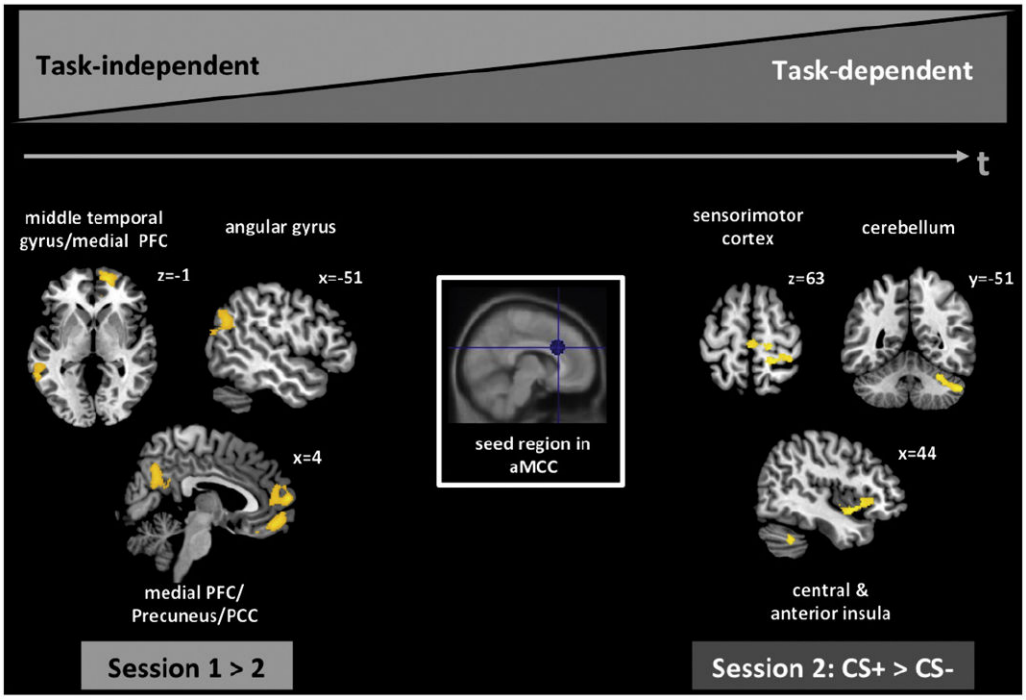

Fig. 4.

Task-dependent and -independent connectivity of the aMCC across sessions was assessed by psychophysiological interaction (PPI) analysis. Using a 10 mm sphere around the peak voxel at [8 23 29], significant coupling of the aMCC with other voxels throughout the entire brain was determined across sessions, and in dependence or independence of CS-conditions (CS+, CS−). Using a cluster-correction procedure, task-unspecific coupling was only found during the first session, including the left middle temporal and right angular gyrus, bilateral medial prefrontal cortex (PFC), as well as bilateral posterior cingulate cortex (PCC). No cluster appeared to be significantly correlated in a task-unspecific manner during the second session. In contrast, while no cluster was found to show task-specific connectivity with the aMCC during the first session, a network including the right sensorimotor cortex, insula and cerebellum was significantly correlated with the aMCC, whichwas specific for the CS +condition. No such couplingwas observed for the CS−condition in the second session.

Table 1

Differential brain activation in CS+ and CS− conditions across sessions.

	Size (k)	x	y	z	Brain regions	H	T
Session 1, CS+ > CS −	No suprathreshold voxel						
Session 1, CS− > CS+ Temporal	55	38	12	−35	Middle temporal pole (BA 38)	R	5.61
Session 2, CS+ > CS− Cingulate/Frontal	5913	29	45	32	Middle frontal and dorsomedial superior frontal gyrus (BA 8/9/10), aMCC/pMCC (BA 24/32), SMA (BA 6)	LR	7.19
		8	23	29	aMCC (BA 32)	R	6.25
	386	3	−36	29	Posterior cingulate cortex (BA 23)	LR	6.77
	62	−11	18	29	aMCC (BA 24/32)	L	5.69
	97	−35	47	24	Middle frontal gyrus (BA 10)	L	5.54
Insula/Operculm	398	54	21	−2	Frontal operculum (Area 44), IFG p. triangularis (BA 45), inferior OFC (BA47)	R	6.16
Sensorimotor	855	−8	−5	71	SMA, paracentral lobule (BA 6)	LR	6.60
	692	−41	−2	53	Ventral premotor area (BA 6)	L	6.16
Temporal	476	68	−47	15	Superior/middle temporal gyrus (BA 22)	R	6.80
	301	−54	15	−9	Superior temporal pole (BA 38)	L	5.99
	265	−60	−44	21	Superior and middle temporal gyrus (BA 22), supramarginal gyrus (PF)	L	5.52
	126	50	−62	−18	Inferior temporal gyrus (BA 37)	R	5.49
	74	69	−35	−8	Middle temporal gyrus (BA 21)	R	5.48
Parietal	1516	2	−72	48	Precuneus, superior parietal lobule (7P, 7M, 5L)	LR	6.17
	299	−54	−54	39	Supramarginal gyrus (PFm)	L	6.26
	136	−38	−56	54	Superior parietal lobule (7A, 7PC)	L	5.65
	84	45	−54	48	Angular and supramarginal gyrus (PGa, PFm)	R	5.23
Occipital	357	23	−98	−14	Lingual gyrus (Area 17, Area 18, hOC3v V3)	R	6.17
	103	42	−86	−12	Inferior occipital gyrus (hOC4v)	R	5.88
	180	33	−63	−14	Fusiform gyrus (BA 19)	R	5.85
	154	−27	−60	−17	Fusiform gyrus (BA 19)	L	5.81
	77	−36	−87	12	Middle occipital gyrus (BA 19)	L	5.67
	67	−32	−90	−18	Lingual gyrus (hOC4v V4)	L	5.46
	135	8	−89	−5	Lingual gyrus (BA 17)	R	5.17
Subcortical	130	−8	−14	8	Thalamus (prefrontal; MD, VL)	L	5.90
	96	6	−11	5	Thalamus (prefrontal; MD, VL)	R	5.80

	Size (k)	x	y	z	Brain regions	H	T
Session 2, CS− > CS+	No suprathreshold voxel						

Notes: T-contrasts were inclusively masked with the interaction term at a threshold of $p_{uncorr} < .001$ (voxel level), and activation was reported at a threshold of $p_{corr} < .05$ (voxel level, FWE corrected for multiple comparisons), using a cluster extend threshold of k = 50; x-, y-, and z-coordinates (MNI) refer to the voxel showing maximal activation in the corresponding cluster; the peak voxel within the right aMCC as part of the biggest cluster (k = 5913) is additionally reported, as it serves as seed region in the later PPI analysis. 'Brain region' gives a detailed list of involved brain structures, which were anatomically classified according to the SPM Anatomy toolbox or AAL atlas (see Material and methods).

Abbreviations: BA: Brodmann area, aMCC: anterior midcingulate cortex, pMCC: posterior midcingulate cortex, IFG: inferior frontal gyrus, OFC: orbitofrontal gyrus, SMA: supplementary motor area, MD: mediodorsal nucleus of the thalamus, VL: ventrolateral nucleus of the thalamus.

Table 2

Differential, task-dependent and -independent connectivity of the aMCC seed region [8 23 29] across sessions.

Cluster	Size (k)	x	y	z	Brain regions	H	T
Task-independent connectivity							
Session 1 > session 2 Frontal	3161	14	60	2	Medial superior frontal gyrus (BA 10), superior and medial OFC (BA 10/11), rectal gyrus (BA 11), pg/sgACC (BA 32)	LR	6.36
Cingulate	1341	−11	−53	30	dPCC/vPCC (BA 23/31), Precuneus (BA 31/7)	LR	5.20
Temporal	636	−62	−41	−8	Middle temporal gyrus (BA 21)	L	4.79
Parietal	702	−51	−63	30	Angular gyrus (PGa)	L	4.45
Session 2 > session 1	No suprathreshold cluster						
Task-dependent connectivity							
PPI session 1, CS+ > CS−	No suprathreshold cluster						
PPI session 1, CS− > CS +	No suprathreshold cluster						
PPI session 2, CS+ > CS−							
Subcortical	598	53	−51	−41	Cerebellum (Lobule VIIa Crus I, VI)	R	4.61
Sensorimotor	647	21	−41	63	Postcentral gyrus (Area 1, 2, 3b), precentral gyrus (Area 4p), paracentral lobule and SMA (Area 6)	R	4.79
Insula	475	42	5	−11	Ventral central insula (BA 13), anterior insula (BA 13)	R	4.43
PPI session 2, CS+_ >CS+	No suprathreshold cluster						

Notes: For analysis of task-independent connectivity of the aMCC seed region, t-contrasts were thresholded at $p_{uncorr} < .001$ (voxel level). For analysis of task-dependent connectivity of the aMCC seed region, t-contrasts were inclusively masked with the interaction term at a threshold of $p_{uncorr} < .05$ (voxel level), and thresholded at $p_{uncorr} < .001$ (voxel level). Activation was reported in clusters surviving cluster-level correction at $p_{corr} < .05$ (FWE corrected for multiple comparisons); x-, y-, and z-coordinates (MNI) refer to the voxel showing maximal activation in the corresponding cluster; 'Brain region' gives a detailed list of involved brain structures, which were anatomically classified according to the SPM Anatomy toolbox or AAL atlas (see Material and methods).

Abbreviations: BA: Brodmann area, aMCC: anterior midcingulate cortex, dPCC: dorsal posterior cingulate cortex, vPCC: ventral posterior cingulate cortex; pg/sgACC: pre- and subgenual anterior cingulate cortex, OFC: orbitofrontal gyrus, SMA: supplementary motor area.